Combined effects of ECAP and subsequent heating parameters on semi-solid microstructure of 7075 aluminum alloy

Ramin MESHKABADI[1], Ghader FARAJI[1], Akbar JAVDANI[2], Vahid POUYAFAR[2]

1. School of Mechanical Engineering, College of Engineering, University of Tehran, Tehran 11155-4563, Iran;
2. Department of Mechanical Engineering, University of Tabriz, Tabriz 5166616471, Iran

Abstract: The combined effects of equal channel angular pressing (ECAP) and subsequent heating to a semi-solid temperature on the microstructural characteristics of the 7075 aluminum alloy were investigated. The microstructure is influenced by several parameters including the number of ECAP passes, ECAP route, consequent heating temperature, and holding time. The effects of these parameters on the microstructural characteristics including grain size and shape factor of the 7075 aluminum alloy were studied using experimental tests and Taguchi method. The results indicate that five-pass ECAP in route B_A and subsequent isothermal holding at 630 °C for 15 min are more appropriate for achieving a semi-solid microstructure. The processing route and holding time have the highest impact on the grain size while the number of ECAP passes and heating temperature have the least impact on the grain size. Meanwhile, the shape factor is significantly influenced by the processing route, holding time and heating temperature while it is less influenced by the number of ECAP passes.

Key words: 7075 aluminum alloy; equal channel angular pressing; semi-solid microstructure; grain size; shape factor

1 Introduction

Semi-solid metal processing is a near net shape manufacturing process for metals and alloys which takes place at temperatures between the solidus and the liquidus [1]. To benefit from the flow behavior of materials in semi-solid forming, the solid phase should have a globular structure dispersed in a liquid matrix. There are various routes to obtain non-dendritic microstructures before semi-solid forming, such as magneto hydro dynamic (MHD) stirring, thermo-mechanical processing like strain induced melt activated (SIMA) and recrystallization and partial melting (RAP) methods, which are similar but distinct [2]. The 7075 wrought aluminum alloy is widely used for high-strength structural applications such as aircraft and automotive parts. The semi-solid forming of this alloy close to net shape is of more importance because it is mostly formed by a costly machining process [3−5].

Up to now, some researchers have conducted investigations about the microstructural evolution of 7075 aluminum alloy produced by SIMA and RAP methods. SANG et al [6] investigated the effects of cold working and heating conditions on the microstructure of this alloy in the SIMA process. They found that at least 50% cold working was necessary to obtain a uniform microstructure during semi-solid heating.

ATKINSON et al [7] examined the formation of spheroids in as-supplied 7075 aluminum alloy. They reheated 7075 alloy in the extruded and T6 condition into the semi-solid state. Fully spherical microstructures were obtained on reheating as-supplied material to temperatures approaching 580 °C, although the fractions of liquid at that temperature were still low at around 5%.

BOLOURI et al [8,9] investigated the effects of compression rate on the microstructure evolution of semi-solid 7075 aluminum alloy produced by the SIMA process. The samples were cold deformed by compression to an extent up to 40% reduction. Their results revealed that the average grain size was gradually reduced as the compression rate increased.

The semi-solid slurry of aluminum alloys was prepared by a serpentine pouring channel (SCP) and the influences of pouring temperature and the number of turns on the microstructure of semi-solid alloy were

investigated [10−12]. The results demonstrated that the semi-solid 7075 alloy slurry with a satisfactory quality could be generated by a serpentine pouring channel. By using this method, they achieved the value of 0.78 for shape factor [10]. MOHAMMADI et al [13] studied microstructural evolution during partial remelting of 7075 aluminum alloy by using the RAP method to obtain a semi-solid feedstock for semi-solid forming. Results showed that a fine and globular microstructure can be obtained by the RAP route. Also, a high semi-solid isothermal temperature would increase the liquid volume fraction and accelerate the spherical processing of solid particles. Furthermore, at a longer holding time, the globular grains coarsened slightly and the average grain sizes increased. WANG et al [14] studied the effects of the isothermal holding process on the microstructure evolution of semi-solid 7075 aluminum alloy produced by RAP process. The results showed that the microstructure of as-received alloy exhibited a remarkable orientation along the deformation direction. Along with the increase of isothermal holding time, the solid particle grain size increased continuously, and the degree of spheroidization improved. ASHOURI et al [15] used the ECAP process for one to four passes to examine the effects of strain on the morphology and shape factor of reheated A356 alloy. Their conclusions indicated that with an increase of strain, the sphericity of particles increased, their size decreased, and sphericity took place in less reheating time. HOSSEIN NEDJAD et al [16] reported that partially melted dendritic cast structure underwent substantial plastic deformation during semisolid equal channel angular press. Coarsening of the fragmented dendritic microstructure during subsequent semisolid isothermal heating gave rise to spheroidal solid phase surrounded by liquid metal. JIANG et al [17] investigated the microstructural evolution of AZ61 magnesium alloy deformed by ECAP during semisolid isothermal treatment. The results show that extrusion pass, isothermal temperature, and processing route have an influence on the microstructural evolution of preformed AZ61 magnesium alloy during semi-solid isothermal treatment.

Initial feedstock preparation plays an important role in the characteristics of the final product. To overcome the restrictions of traditional SIMA methods like inhomogeneity and the amount of strain in every pass, ECAP is used as a strain-inducing process in the present study. The concentrations in the previous investigations of this alloy lie on the influence of each parameter individually, but a study that considers the combinational effects of parameters cannot be seen in the literature. In this research, the combined effects of selected ECAP and subsequent reheating parameters on the semi-solid microstructure of 7075 aluminum alloy were evaluated thoroughly by using Taguchi method [18]. The other issue which was not addressed in previous studies is that it is of importance to determine the optimum conditions for the best microstructure, and the contribution percentage of any parameter on the resulting microstructure when ECAP is applied. The current study alleviates the problems mentioned.

2 Experimental

The chemical composition of as-received 7075 aluminum alloy is shown in Table 1. Wrought aluminum alloys are difficult to be processed by ECAP at room temperature because they fail by catastrophic cracking due to coarse precipitates and dendritic structures [19]. It is necessary to use an appropriate heat treatment to reduce the hardness of the samples before applying the deformation process [20]. To do so, cylindrical samples with 20 mm in diameter and 70 mm in height were machined from as-received ingots and annealed at 320 °C for 2 h, and then furnace-cooled to room temperature. To impose deformation on the samples, the designed ECAP die with two equal cross-section channels (20 mm in diameter) and channel angle of $\Phi=90°$ and an outer curvature angle of $\Psi=20°$, was used as illustrated in Figs. 1(a) and (b) [21]. The pressing speed was 5 mm/s, and the process was done at room temperature. Samples were lubricated by MoS_2 to reduce friction between the die and sample during the process.

Table 1 Chemical composition of 7075 aluminum alloy (mass fraction, %)

Zn	Mg	Cu	Cr	Mn	Fe	Si	Al
5.27	2.25	1.51	0.229	0.139	0.405	0.333	Bal.

A PID-controlled resistance furnace was used to heat the samples, and the temperature of the slug was monitored by a K-type thermometer system. Since the heating time in our experiments is short, we should consider the required time to reach the steady-state temperature. Thus, the heating curve of the sample was recorded as presented in Fig. 2. The curve shows that the average heating rate of the sample is 2.5 °C/s, and the temperature reaches the semi-solid zone after about 6 min. This should be added to the holding time.

After heating the ECAP-treated samples to a predetermined temperature and holding for a required time, they were quenched in cold water. To investigate the microstructure, the cross sections of the samples were polished and then etched using Keller's solution. The microstructures were observed using an optical microscope (OM). Image analysis software was used to determine the grain size (d) and shape factor (S_F) of the microstructures using Eqs. (1) and (2):
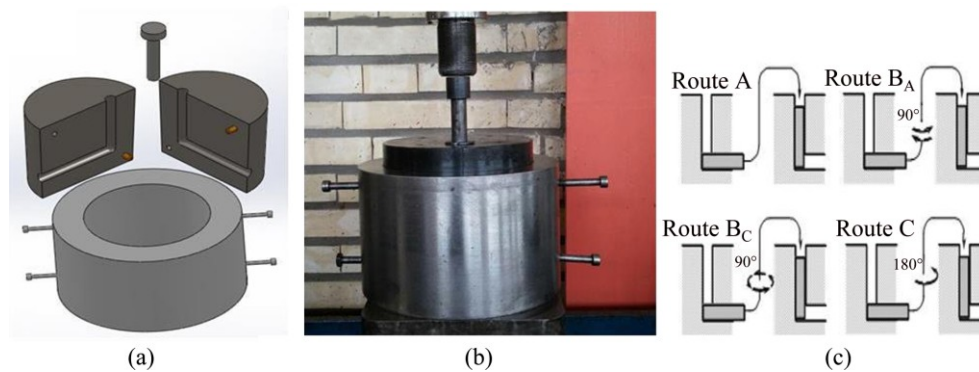
Fig. 1 Schematic illustration of ECAP die (a), ECAP die set-up (b) and four fundamental pressing routes in ECAP (c) [21]
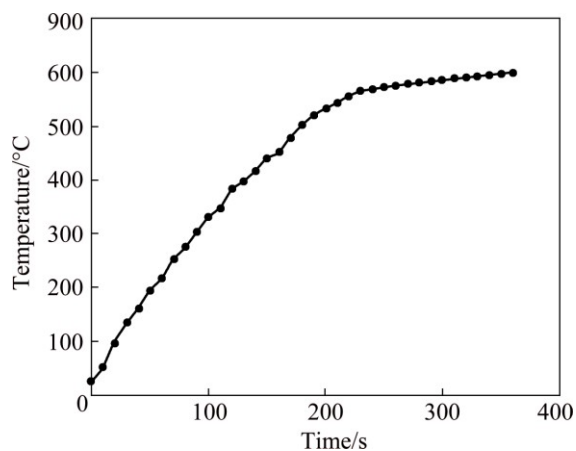

Fig. 2 Heating curve of sample in resistance furnace

$$d = \frac{\sum_{1}^{N} \sqrt{4A/\pi}}{N} \qquad (1)$$

$$S_{\mathrm{F}} = \frac{1}{\sum_{1}^{N} [P^2 N/(4\pi A)]} \qquad (2)$$

where A is the surface area of the particle, P is the perimeter of the particle, and N is the number of particles in the selected area of the images [22].

3 Design of experiments

An appropriate microstructure for semi-solid forming depends on the parameters of the strain inducing method and subsequent semi-solid heating approach. We can classify the input parameters as ECAP and semi-solid heating parameters. The examined output parameters in this study are grain size and shape factor which are determinative in the semi-solid forming process.

3.1 Determination of ECAP parameters

Based on the conducted surveys on aluminum alloys, the effective ECAP parameters are processing route, number of passes, forming speed and forming temperature. Among them, the forming speed and temperature have almost no significant effect on the final microstructure [22]. Thus, they will not be examined in this study. So, four possible processing routes (A, B_A, B_C and C as displayed in Fig. 1(c)), and different numbers of passes (2, 3, 4 and 5) were selected as ECAP parameters.

3.2 Determination of semi-solid heating parameters

The desired levels of heating temperatures were chosen to include low, medium, and high liquid fractions. Therefore, the heating temperatures (605, 615, 620 and 630 °C) were selected based on liquid fractions (20%, 30%, 40% and 60%) from the DSC curve of the alloy. Additionally, the liquid fraction of the samples determined by image analyzing software and the obtained results are shown in Fig. 3, which accord with DSC results.
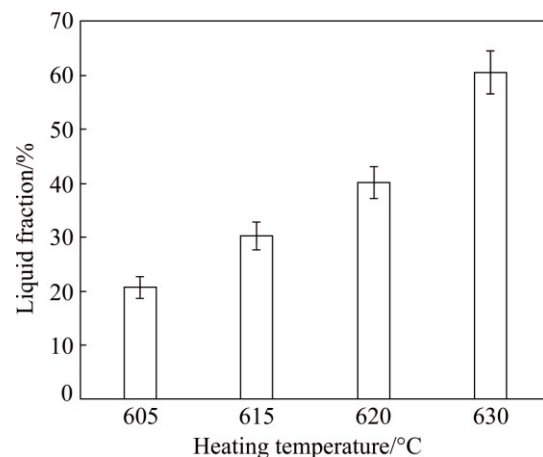

Fig. 3 Liquid fractions at desired heating temperatures by image analysis

A one-pass ECAP-processed sample was heated at 595 °C and quenched after holding time of 5, 10, 15, 20, 30 and 40 min to determine the effectiveness of holding time. The microstructure evolution of the sample, the measured grain size and shape factor are shown in Figs. 4 and 5, respectively. Since a suitable microstructure for any semi-solid forming process must
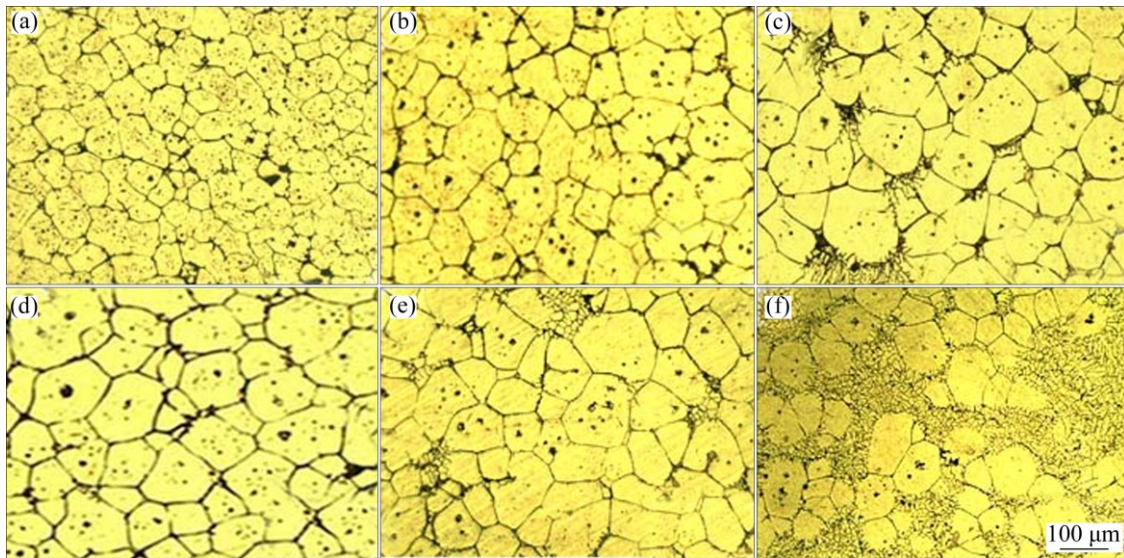
Fig. 4 Microstructure evolution of one-pass ECAP-treated sample at 595 °C for different holding time: (a) 5 min; (b) 10 min; (c) 15 min; (d) 20 min; (e) 30 min; (f) 40 min
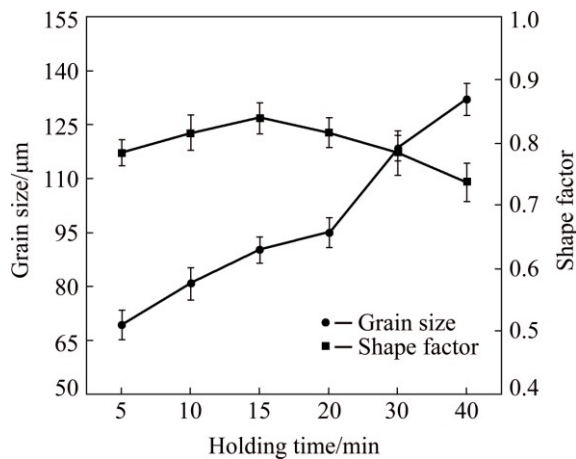

Fig. 5 Variations of grain size and shape factor based on holding time at 595 °C for one-pass ECAP-treated sample

have a grain size of 70−100 μm [23], it is revealed that when the holding time increases up to 20 min, the grain size is about 100 μm and then increases excessively. So, holding for more than 20 min at the desired temperature is not appropriate for a semi-solid process. Shape factor is not influenced by holding time prominent up to 20 min, and decreases after that. According to the above considerations, the holding time levels were chosen to be 5, 10, 15, and 20 min, respectively.

3.3 Taguchi method and analysis of variance (ANOVA)

Table 2 shows the factors and four different levels for each of them. As a result, the full factorial design requires numerous experiments to be carried out as mentioned above. To overcome this problem, Taguchi method was employed to reduce the required experiments. The most suitable orthogonal array of experimentation is L_{16}, as shown in Table 3.

Table 2 Factors and their levels

Factor	Level 1	Level 2	Level 3	Level 4
Route	A	B_A	B_C	C
Number of passes	2	3	4	5
Heating temperature /°C	605	615	620	630
Holding time/min	5	10	15	20

Table 3 Design of experiments by L_{16} array

Experiment No.	Route	Number of passes	Heating temperature/°C	Holding time/min
1	A	2	605	5
2	A	3	615	10
3	A	4	620	15
4	A	5	630	20
5	B_A	2	615	15
6	B_A	3	605	20
7	B_A	4	630	5
8	B_A	5	620	10
9	B_C	2	620	20
10	B_C	3	630	15
11	B_C	4	605	10
12	B_C	5	615	5
13	C	2	630	10
14	C	3	620	5
15	C	4	615	20
16	C	5	605	15

To investigate the effect of parameters on the specified output of the process, analysis of variance (ANOVA) [18] is a common statistical method. ANOVA helps for determining the significance of all factors and their interactions by applying the results of the experiment. It also determines which of input parameters need to be controlled and which do not. Equation (3) was used to determine the contribution percentage (P_c) of each parameter on the results.

$$P_c = \frac{S_{si} - D_{ofi}M_{se}}{S_{st}} \times 100\% \tag{3}$$

where S_{si} is the sum of squares; D_{ofi} is the degree of freedom; M_{se} is the mean square error, and S_{st} is the total sum of squares. Finally, the schematic procedure in this study is illustrated in Fig. 6.

4 Results and discussion

As mentioned above, experiments were conducted according to the condition shown in Table 3. The resultant microstructures are shown in Fig. 7. Note that the liquid content apparent in the micrographs of microstructures is not indicative of the exact quantity presented at that temperature because the quenching is not sufficiently rapid for the liquid content to be entirely "frozen in". During the quenching experiments, some liquid phases were deposited onto the existing solid surfaces, appearing to be "solid" in the quenched microstructures [8]. The grain size and shape factor were measured in at least 15 different locations and the average values for each experiment are shown in Table 4.
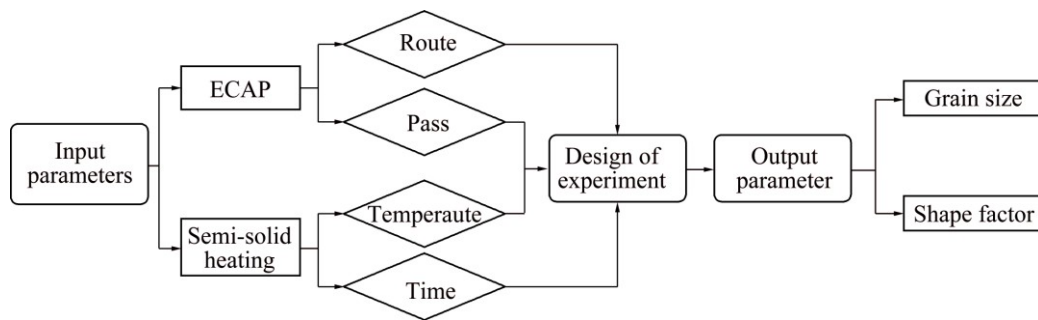

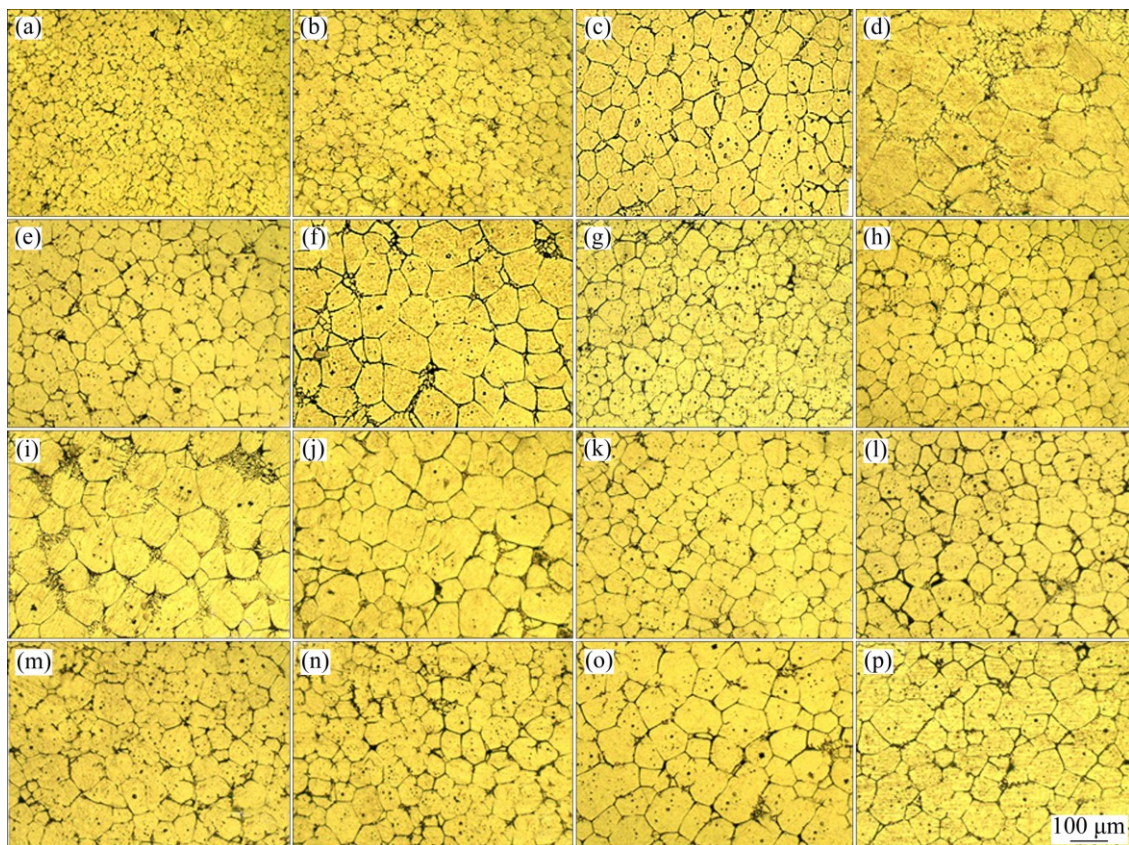**Fig. 6** Schematic illustration of input and output parameters

Fig. 7 Microstructures for all experiments ((a−p) corresponding to experiments No.1−16 in Table 3, respectively)

Table 4 Measured values of grain size and shape factor

| Experiment No.	Shape factor	Grain size/μm
1	0.63	58
2	0.68	62
3	0.77	79
4	0.85	91
5	0.80	75
6	0.82	79
7	0.77	66
8	0.85	64
9	0.82	107
10	0.85	87
11	0.75	91
12	0.75	80
13	0.69	98
14	0.64	92
15	0.73	115
16	0.71	97

Two other experiments were also conducted as the verifiers of the Taguchi analysis method, and the results are shown in Table 5. The prediction of the Taguchi design approach is in a good agreement with experimental results while the mean error of it is about 2%.

Considering that the aim is to evaluate the value and impact of input parameters on the output parameters, and also to determine optimal levels of each parameter, the variations are considered by a factor called signal-to-noise ratio (S/N). The S/N ratio measures the performance characteristics of the process and helps to reduce its variance and prevent its deviation from the target value. The criteria of "the smaller the better" for grain size and "the larger the better" for shape factor are considered in selecting the S/N ratio to create the highest amount of responses.

The level which results in the highest value of S/N ratio is chosen as the optimal level of a process parameter. In fact, the S/N ratio indicates that the effectiveness of controllable factors is better than that of uncontrollable and disturbance factors. Figures 8 and 9

Table 5 Confirmation experimental results obtained by Taguchi analysis

Experiment No.	Experiment condition	Grain size			Shape factor		
		Measured/μm	Predicted/μm	Error/%	Measured	Predicted	Error/%
1	Route A, 3 passes 630 °C, 5 min	58	60	3	0.69	0.70	1.5
2	Route B_A, 2 passes 605 °C, 20 min	82	83	1	0.78	0.80	2.5
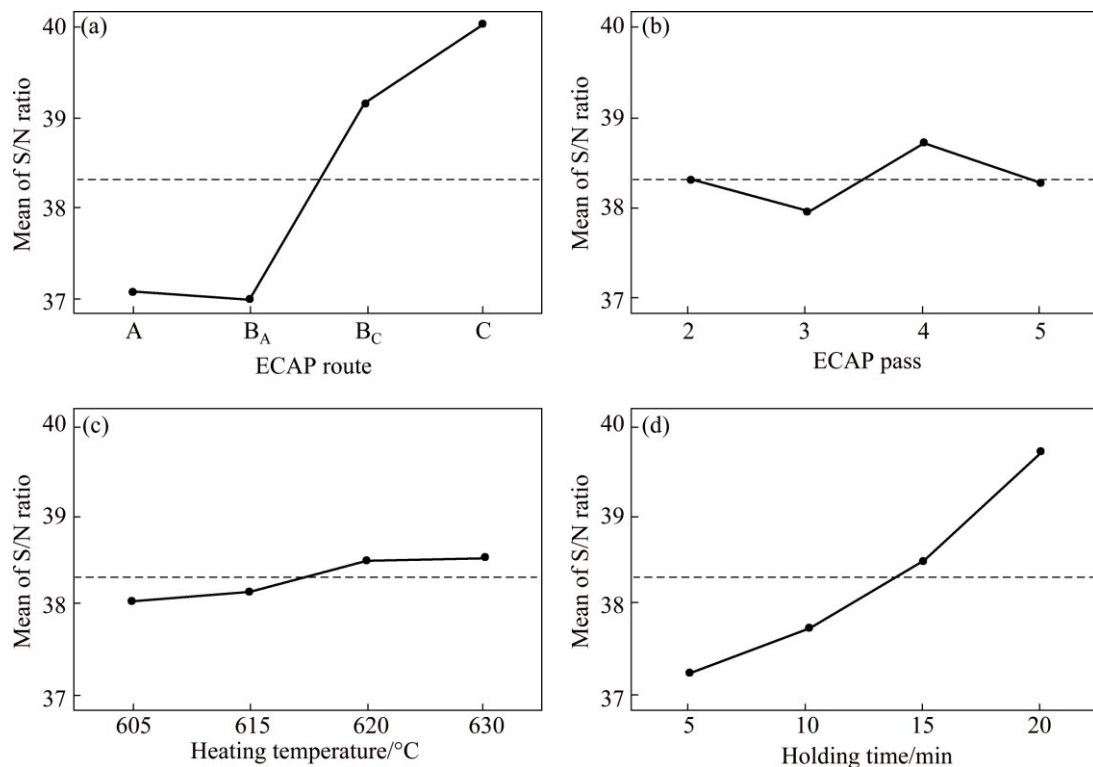
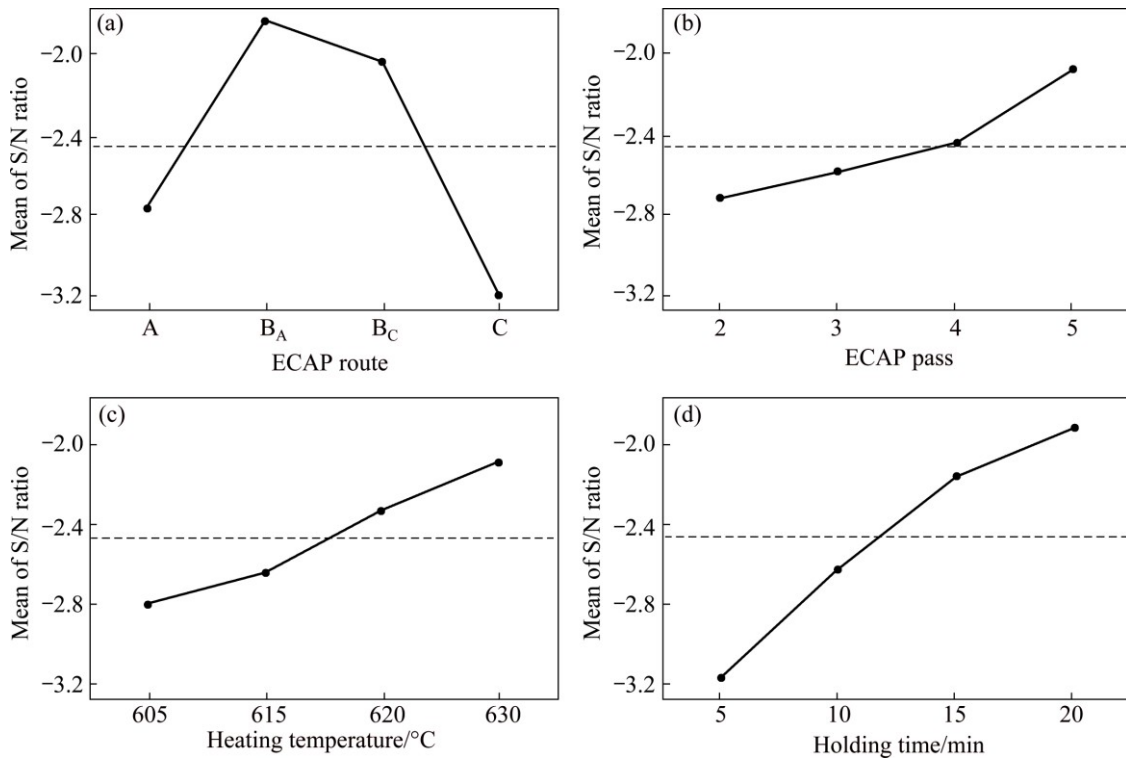**Fig. 8** S/N ratio analysis of grain size

Fig. 9 S/N ratio analysis of shape factor

show the S/N ratio versus parameter level diagrams for grain size and shape factor, respectively.

By analyzing the figures, the optimal conditions that satisfy both grain size and shape factor include ECAP processing in route B_A up to five passes and heating at 630 °C for 15 min. The predicted shape factor and grain size of the optimal parameters are 0.87 and 66 μm, respectively, which are suitable for semi-solid forming. The obtained optimum shape factor value is improved in comparison with the results of the serpentine pouring channel (SCP) method used by ZHU et al [10]. The resultant microstructure of the optimal parameters is shown in Fig. 10.
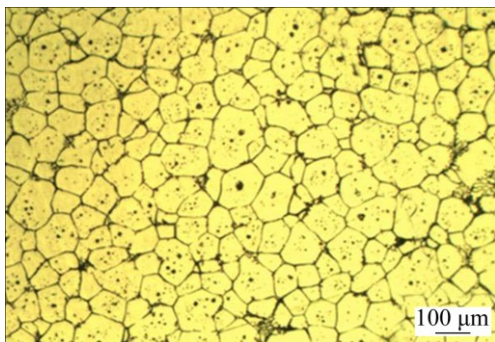

Fig. 10 Microstructure of optimal conditions resulting from Taguchi method (B_A, 5 passes, 630 °C, 15 min)

Based on the results of Taguchi analysis, the variations of each parameter are plotted by assuming a

constant average for other parameters. Figure 11 shows the variation of grain size as a function of ECAP and heating parameters.

Referring to Fig. 11(a), different processing routes have different influences on grain size. The reason can be justified based on the fact that different routes represent various slip systems, leading to fundamental changes in the produced microstructure by ECAP process. As shown in Fig. 12 [21], the applied shear stress in different passes continues on the same plane for ECAP processing in route C. So, the direction of the imposed strain in each pass is reversed, and the strain after an even number of passes is restored. In route B_C, the strain in the first pass is restored by the third pass, and the strain in the second pass is restored by the fourth pass as well. By examining the slip planes on routes A and B_A, it can be seen that route A has two different slip planes intersecting at an angle of 90° and route B_A has four distinct slip planes intersecting at an angle of 120°. On these routes, in each pass, the strain amount is added to the previous amount, and there would not be afterwards [21].

Figure 11(a) shows that variation of the number of passes has a little influence on grain size. By applying a severe plastic deformation, strain energy is stored in the structure of the alloy and, as the deformation increases, the stored strain energy is increased up to a critical value. According to Ref. [8] which presented the effects of compression rate and mushy zone on the thixotropic microstructure of 7075 alloy, when the compression ratio

surpasses 30%, the stored strain energy reaches its critical value. When a critical value is reached, the accumulated rate of strain energy descends as deformation goes on. This results in the reduced effect of recrystallization in the final microstructure. In our case, the equivalent compression rate after the first pass ECAP is equivalent to 100% [21] and according to the descriptions above, passes exceeding one have no effect on variations of the recrystallization and grain size.
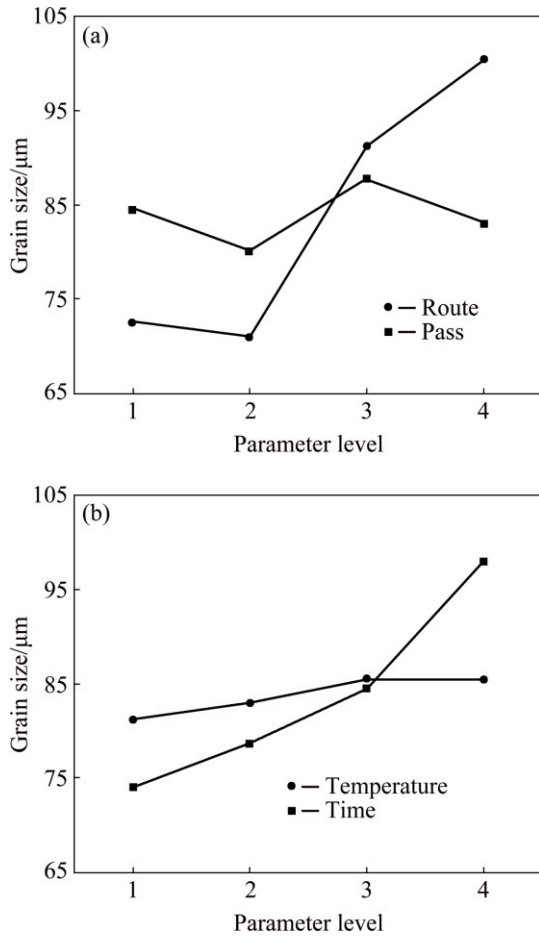

Fig. 11 Variations of grain size as function of ECAP input parameters (a) and heating parameters (b)

As observed in Fig. 11(b), increasing the heating temperature causes a slight change in the grain size, because when the liquid content increases, the combination of small solid grains becomes difficult and the grain size does not change anymore. Figure 11(b) shows that by increasing the holding time, the grain size increases. The reason can be justified based on the Ostwald ripening mechanism, dominant in a long time and at a high liquid fraction [24]. These trends were also observed by MOHAMMADI et al [13] and WANG et al [14] in obtaining a semi-solid feedstock by the RAP method.

Figure 13 displays the variations of shape factor versus input parameters (ECAP and heating parameters).
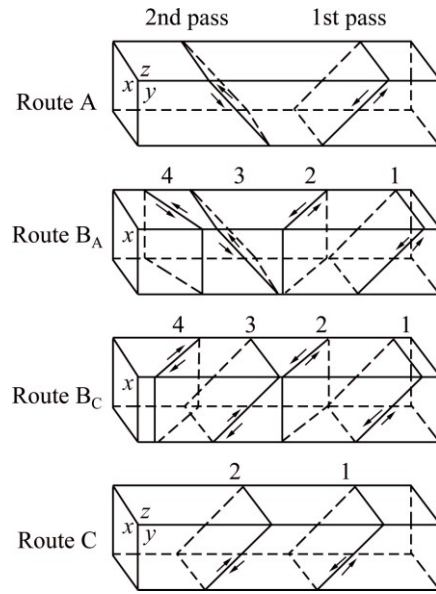

Fig. 12 Slip systems for successive passes in different processing routes [21]
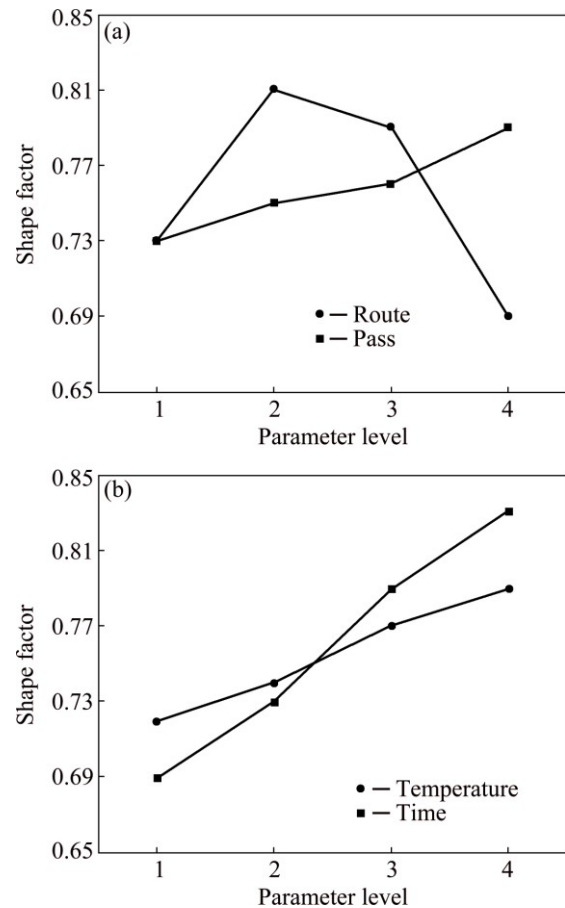

Fig. 13 Variations of shape factor as function of ECAP input parameters (a) and heating parameters (b)

Considering the effects of the processing routes on the shape factor, ECAP-processed samples via routes B_A and B_C have the highest globularity. However, it has reduced value in ECAP-processed samples via routes A and C

(Fig. 13(a)). Additionally, by increasing the number of passes from 2 to 3, the globularity is almost remained unchanged. After changing the number of passes from 4 to 5 passes, it improves and reaches about 0.80. In fact, when the number of passes increases, the stored energy in sample increases and as a result, the large amount of induced strain energy promotes globularization.

As displayed in Fig. 13(b), the variation of shape factor as a function of heating temperature is increasing. The maximum value of shape factor was obtained at 630 °C. When the temperature is raised, and a sufficient molten phase is formed, high-energy grain boundaries are penetrated by liquids, leading to the fragmentation of original grains to small equiaxed ones. However, the presence of molten phase causes grain growth and spheroidization of the newly formed grains [25]. The influence of holding time is more prominent because when holding time increases, the shape factor increases as a result of decreasing the surface energy of solid particles with diminishing sharp edges.

For precise evaluation, the contribution percentage of individual parameters on the grain size and shape factor was examined by analysis of variance using Minitab software. ANOVA results of the experimental tests for the grain size and shape factor are presented in Tables 6 and 7, respectively. This analysis was performed at a level of significance of 5%, i.e., for a level of confidence of 95%. Table 6 indicates that the P-values of processing routes and holding time are less than α (0.05)

value. This means that these parameters are statistically significant. From the ANOVA results (Table 7), it can be seen that the effects of process parameters such as processing route and heating temperature and time are important as their statistically significant values are less than α (0.05) value at 95% confidence level.

The contribution percentage of input parameters on grain size and shape factor is calculated by using Eq. (3) based on the presented results in Tables 6 and 7. The calculated percentage shown in Fig. 14 indicates that the most influential process parameters on grain size are processing route (60% contribution) followed by holding time (30% contribution). The number of passes and heating temperature have a little influence (2% contribution) on the grain size when the combinational effect is considered. Some other process parameters have also affected the process but were not investigated here. They were pressing speed, pressing temperature, frictional effects, and other uncontrollable parameters whose effectiveness of 6% was a tolerable value regarding Taguchi approach.

The obtained results of shape factor in Fig. 14 show that the most effective parameters are processing route

Table 6 ANOVA results for S/N ratio for grain size

Source	DF	Seq. SS	Adj. MS	F	P-value
Route	3	2503.69	834.56	30.65	0.009
Number of passes	3	124.69	41.56	1.53	0.368
Heating temperature	3	51.69	17.23	0.63	0.642
Holding time	3	1294.69	431.56	15.85	0.024
Error	3	81.69	27.23		
Total	15	4056.44			

Table 7 ANOVA results for S/N ratio for shape factor

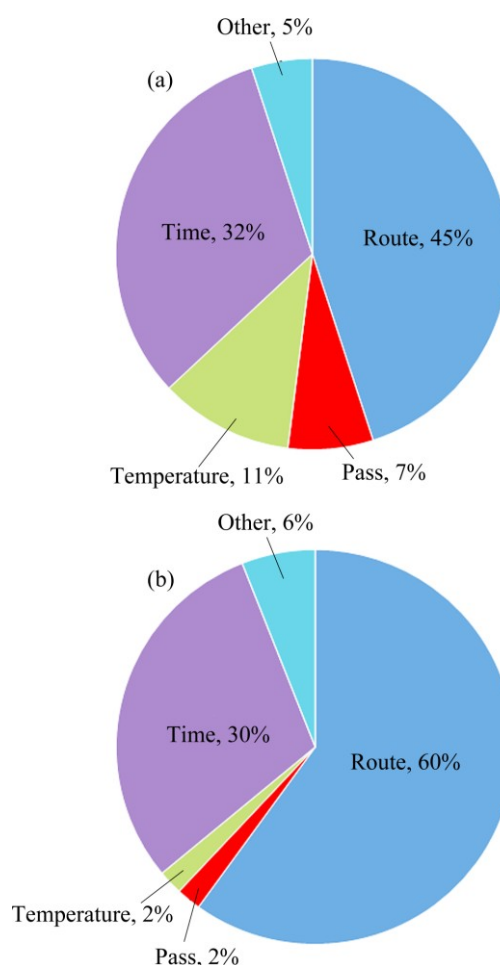| Source	DF	Seq. SS	Adj. MS	F	P-value
Route	3	0.0353187	0.0353187	40.65	0.006
Number of passes	3	0.0066687	0.0022229	7.68	0.064
Heating temperature	3	0.0096687	0.0032229	11.13	0.039
Holding time	3	0.0268187	0.0089396	30.87	0.009
Error	3	0.0008687	0.0002896		
Total	15	0.0793437			

Fig. 14 Contribution percentage of process parameters on shape factor (a) and grain size (b)

(45% contribution), followed by holding time (32% contribution), heating temperature (11% contribution) and numbers of passes (7% contribution). In this case, the impact of uncontrollable factors referred above is about 5%. It is important to note that the percentage results were obtained for specified levels of input parameters which were chosen based on the previous explanations to make the results rational.

In either case, the impacts of processing route and holding time are more prominent than others, and they should be considered in the production of a suitable feedstock for semi-solid forming of this alloy. Also, the low impact of other parameters (forming speed and temperature) confirms the presented results by VALIEV and LANGDON [21].

5 Conclusions

1) A combination of ECAP and subsequent heating to semi-solid temperature has a good potential to make 7075 aluminum alloy more suitable for semi-solid forming. By applying a proper heat treatment, ECAP is done up to five passes without any crack or fracture. The microstructures of processed and isothermally held alloy in the semi-solid zone contain round solid grains surrounded by liquid films.

2) The L_{16} Taguchi orthogonal design of experiments was conducted successfully, and the microstructural characteristics of the semi-solid alloy were investigated by considering the combined effects of ECAP and heating parameters.

3) Since higher shape factor and smaller grain size are more favorable in semi-solid forming, the most suitable microstructure is obtained by processing in route B_A up to five passes and then heating at 630 °C for 15 min.

4) The prediction made by the Taguchi design approach is in good agreement with experimental results.

5) Regarding the ANOVA results, processing routes and holding time with the minimum possible P-values are the most effective terms to obtain a smaller grain size. When the combined effect is taken into account, the number of passes and heating temperature do not show any significant effects on the grain size.

6) The shape factor is mostly influenced by processing routes, heating temperature and holding time. When combined effects are taken into consideration, the number of passes does not affect the shape factor.

References

[1]　ATKINSON H V, LIU D. Microstructural coarsening of semi-solid aluminium alloys [J]. Materials Science and Engineering A, 2008, 496: 439−446.

[2]　ATKINSON H V. Modelling the semisolid processing of metallic alloys [J]. Progress in Materials Science, 2005, 50: 341−412.

[3]　SEO P K, KANG C G, LEE S M. A study on reheating characteristics for thixo die casting process with electromagnetic stirring and extruded aluminum alloys and their mechanical properties [J]. The International Journal of Advanced Manufacturing Technology, 2009, 43: 482−499.

[4]　KAMGUEM R, DJEBARA A, SONGMENE V. Investigation on surface finish and metallic particle emission during machining of aluminum alloys using response surface methodology and desirability functions [J]. The International Journal of Advanced Manufacturing Technology, 2013, 69: 1283−1298.

[5]　BHUSHAN R K, KUMAR S, DAS S. Fabrication and characterization of 7075 Al alloy reinforced with SiC particulates [J]. The International Journal of Advanced Manufacturing Technology, 2013, 65: 611−624.

[6]　SANG Y L, JUNG H L, YOUNG S L. Characterization of Al 7075 alloys after cold working and heating in the semi-solid temperature range [J]. Journal of Materials Processing Technology, 2001, 111: 42−47.

[7]　ATKINSON H V, BURKE K, VANEETVELD G. Recrystallisation in the semi-solid state in 7075 aluminium alloy [J]. Materials Science and Engineering A, 2008, 490: 266−276.

[8]　BOLOURI A, SHAHMIRI M, CHESHMEH E N H. Microstructural evolution during semisolid state strain induced melt activation process of aluminum 7075 alloy [J]. Transactions of Nonferrous Metals Society of China, 2010, 20: 1663−1671.

[9]　BOLOURI A, SHAHMIRI M, KANG C G. Study on the effects of the compression ratio and mushy zone heating on the thixotropic microstructure of AA 7075 aluminum alloy via SIMA process [J]. Journal of Alloys and Compounds, 2011, 509: 402−408.

[10]　ZHU Wen-zhi, MAO Wei-min, TU Qin. Preparation of semi-solid 7075 aluminum alloy slurry by serpentine pouring channel [J]. Transactions of Nonferrous Metals Society of China, 2014, 24: 954−960.

[11]　CHENG Shu-jian, ZHAO Yu-hong, HOU Hua, JIN Yu-chun, GUO Xiao-xiao. Preparation of semi-solid ZL101 aluminum slurry by serpentine channel [J]. Transactions of Nonferrous Metals Society of China, 2016, 26: 1820−1825.

[12]　LIU Zhi-yong, MAO Wei-min, WANG Wei-pan, ZHENG Zhi-kai. Preparation of semi-solid A380 aluminum alurry by serpentine channel [J]. Transactions of Nonferrous Metals Society of China, 2015, 25: 1419−1426.

[13]　MOHAMMADI H, KETABCHI M, KALAKI A. Microstructural evolution and mechanical properties of back-extruded Al 7075 alloy in the semi-solid state [J]. International Journal of Material Forming, 2012, 5: 109−119.

[14]　WANG C P, TANG Z J, MEI H S, WANG L, LI R Q, LI D F. Formation of spheroidal microstructure in semi-solid state and thixoforming of 7075 high strength aluminum alloy [J]. Rare Metals, 2015, 34: 710−716.

[15]　ASHOURI S, NILI-AHMADABADI M, MORADI M, IRANPOUR M. Semi-solid microstructure evolution during reheating of aluminum A356 alloy deformed severely by ECAP [J]. Journal of Alloys and Compounds, 2008, 466: 67−72.

[16]　HOSSEIN NEDJAD S, MEIDANI H, NILI AHMADABADI M. Effect of equal channel angular pressing on the microstructure of a semisolid aluminum alloy [J]. Materials Science and Engineering A, 2008, 475: 224−228.

[17]　JIANG Ju-fu, LIN Xin, WANG Ying, QU Jian-jun, LUO Shou-jing. Microstructural evolution of AZ61 magnesium alloy predeformed by ECAE during semisolid isothermal treatment [J]. Transactions of Nonferrous Metals Society of China, 2012, 22: 555−563.

[18] ROSS P. Taguchi techniques for quality engineering: Loss function, orthogonal experiments, parameter and tolerance design [M]. New York: McGraw-Hill, 1996.

[19] CHINH N Q, GUBICZA J, CZEPPE T, LENDVAI J, XU C, VALIEV R Z, LANGDON T G. Developing a strategy for the processing of age-hardenable alloys by ECAP at room temperature [J]. Materials Science and Engineering A, 2009, 516: 248−252.

[20] POKOVA M S, ZIMINA M, CIESLAR M. Effect of pre-annealing on microstructure evolution of TRC AA3003 aluminum alloy subjected to ECAP [J]. Transactions of Nonferrous Metals Society of China, 2016, 26: 627−633.

[21] VALIEV R Z, LANGDON T G. Principles of equal-channel angular pressing as a processing tool for grain refinement [J]. Progress in Materials Science, 2006, 51: 881−981.

[22] JIANG J, WANG Y, QU J, DU Z, SUN Y, LUO S. Microstructure evolution of AM60 magnesium alloy semisolid slurry prepared by new SIMA [J]. Journal of Alloys and Compounds, 2010, 497: 62−67.

[23] ROKNI M R, ZAREI-HANZAKI A, ABEDI H R, HAGHDADI N. Microstructure evolution and mechanical properties of backward thixoextruded 7075 aluminum alloy [J]. Materials & Design, 2012, 36: 557−563.

[24] YANG Bin, MAO Wei-min, SONG Xiao-jun. Microstructure evolution of semi-solid 7075 Al alloy slurry during temperature homogenization treatment [J]. Transactions of Nonferrous Metals Society of China, 2013, 23: 3592−3597.

[25] LOUE W R, SUERY M. Microstructural evolution during partial remelting of Al−Si7Mg alloys [J]. Materials Science and Engineering A, 1995, 203: 1−13.

等通道转角挤压及后续热处理参数对
半固态 7075 铝合金显微组织的影响

Ramin MESHKABADI[1], Ghader FARAJI[1], Akbar JAVDANI[2], Vahid POUYAFAR[2]

1. School of Mechanical Engineering, College of Engineering, University of Tehran, Tehran 11155-4563, Iran;

2. Department of Mechanical Engineering, University of Tabriz, Tabriz 5166616471, Iran

摘　要：研究等通道转角挤压(ECAP)及后续加热到半固态温度对 7075 铝合金显微组织的影响。7075 铝合金的显微组织受 ECAP 道次、ECAP 路径、后续加热温度和保温时间等参数的影响。采用实验及 Taguchi 法探讨上述参数对 7075 铝合金的微观特性包括晶粒尺寸及形状因子的影响。结果表明：5 道次 ECAP、路径 B_A 及后续 630 °C 等温处理 15 min 是合金获得半固态显微组织的较佳工艺条件；加工路径和保温时间对晶粒尺寸的影响最大，而 ECAP 道次和加热温度对晶粒尺寸的影响最小。形状因子受加工路径、保温时间和加热温度的影响较大，而受 ECAP 道次的影响较小。

关键词：7075 铝合金；等通道转角挤压；半固态显微组织；晶粒尺寸；形状因子

(Edited by Wei-ping CHEN)